Assimilation of Ice Concentration and Thickness Data in the Beaufort Sea

C33F-1622

M. Yaremchuk, T. Townsend, G. Panteleev, D. Hebert, and R. Allard

Naval Research Laboratory, Stennis Space Center, MS

U.S. NAVAL RESEARCH LABORATORY

ABSTRACT

Numerical experiments with a regional configuration of the CICE-HYCOM system in the Beaufort Sea assimilating SSMI ice concentration (IC) and CryoSat ice thickness (IT) data acquired in September December of 2015 are presented. We explore sensitivity of the 24-hour IT/IC forecast skill to the system updates, which include introduction of the IT assimilation capability, flow-dependent correlations, and gaussianization of IC innovations. Experiments with IC data assimilation have shown that the flow-dependent correlations provide 5-7% improvement of the forecast skill during the freezing period (10Sept–10Nov) while gaussianization contributes an additional improvement of 3-4% in most of the cases. In winter (11Nov–31Dec) IC assimilation did not produce any statistically significant improvement of the skill due to the loss of dynamical information in the IC fields associated saturation of the ice cover. In contrast, IT assimilation provides larger improvement in November-December compared to October-November due to the better coverage of the Beaufort Sea by observations and their higher relative accuracy in winter. Comparison of the IT forecast fields with independent *in situ* observations by two upward looking sonars demonstrates similar improvements. Much better improvement (10-25%) is observed when comparing IT assimilation runs against monthly means of independent satellite data. Introduction of the heuristic in situ IC/IT correlations into the background covariance model did not produce any improvements of the forecast skill.

METHODOLOGY

1. Inhomogeneous correlation model:

$$\mathbf{Cx} = \mathbf{N}\exp\left[-\frac{1}{2}\nabla^{\mathrm{T}}\mathbf{D}(\boldsymbol{x})\nabla\right]\mathbf{x}$$

$$\mathbf{D} = \hat{\mathbf{D}}^{\mathrm{T}}\hat{\mathbf{D}}: \qquad \hat{\mathbf{D}}(\boldsymbol{x}) = r\begin{bmatrix}\sqrt{\lambda(\boldsymbol{x})} & 0\\ 0 & 1\end{bmatrix}\begin{bmatrix}\cos\theta(\boldsymbol{x}) & \sin\theta(\boldsymbol{x})\\ -\sin\theta(\boldsymbol{x}) & \cos\theta(\boldsymbol{x})\end{bmatrix}$$

$$\nabla^{\mathrm{T}}\hat{\mathbf{D}}\nabla = (\hat{\mathbf{D}}\nabla)^{\mathrm{T}}(\hat{\mathbf{D}}\nabla)$$

2. IC - IT correlation model:

$$\mathbf{C}_{ct} = \begin{bmatrix}\sqrt{\mathbf{C}} & \mathbf{0}\\ \mathbf{0} & \sqrt{\mathbf{C}}\end{bmatrix}\begin{bmatrix}\mathbf{I} & \mathbf{D}_{ct}\\ \mathbf{D}_{ct} & \mathbf{I}\end{bmatrix}\begin{bmatrix}\sqrt{\mathbf{C}} & \mathbf{0}\\ \mathbf{0} & \sqrt{\mathbf{C}}\end{bmatrix}$$

$$D_{ct}(\boldsymbol{x}) = \gamma\{1 - 4[c(\boldsymbol{x}) - 0.5]^2\}$$

3. 2dVar:

$$\delta\mathbf{x} = \mathbf{V}\hat{\mathbf{C}}\hat{\mathbf{H}}^{\mathrm{T}}(\hat{\mathbf{H}}\hat{\mathbf{C}}\hat{\mathbf{H}}^{\mathrm{T}} + \mathbf{I})^{-1}\mathbf{R}^{-1}\delta\mathbf{d} \qquad \hat{\mathbf{H}} = \mathbf{R}^{-1}\mathbf{H}\mathbf{V}$$

4. Univariate Gaussianization:

$$\mathcal{G}(\delta\mathbf{d}) = \mathcal{P}_g{}^{-1}\mathcal{P}_d(\delta\mathbf{d})$$

$$\mathcal{P}_g(\delta d) = \frac{1}{\sqrt{2\pi}}\int_{-\infty}^{\delta d}\exp(-x^2/2)dx = \frac{1}{2}\left(1 + \mathrm{erf}\frac{\delta d}{\sqrt{2}}\right)$$

$$\mathcal{G}^{-1}(\delta\mathbf{x}) = \mathcal{P}_d{}^{-1}\left[\frac{1}{2}(1 + \mathrm{erf}\frac{\delta\mathbf{x}}{\sqrt{2}})\right]$$

EXPERIMENT SETTING

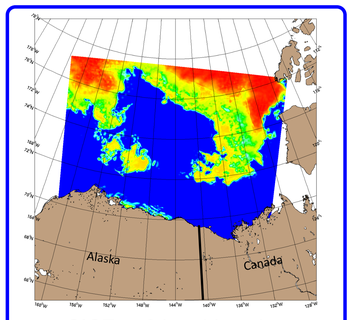

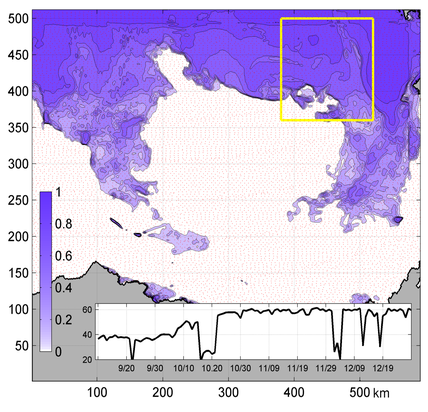

CICE at 2 km driven by:
NAVGEM 1.2 forcing
and GOFS 3.1
(1/12° HYCOM/NCODA)
Assimilation period:
9/2/2015-12/31/2015

Forecast skill assessment: $s^n(a|r) = 1 - \dfrac{(\mathbf{Hx}_a^n - \mathbf{d}^n)^{\mathrm{T}}(\mathbf{Hx}_a^n - \mathbf{d}^n)}{(\mathbf{Hx}_r^n - \mathbf{d}^n)^{\mathrm{T}}(\mathbf{Hx}_r^n - \mathbf{d}^n)}$

IMPACT OF FLOW-DEPENDENT CORRELATIONS

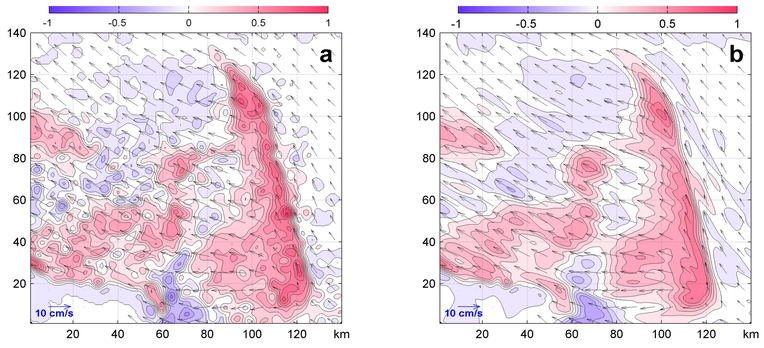

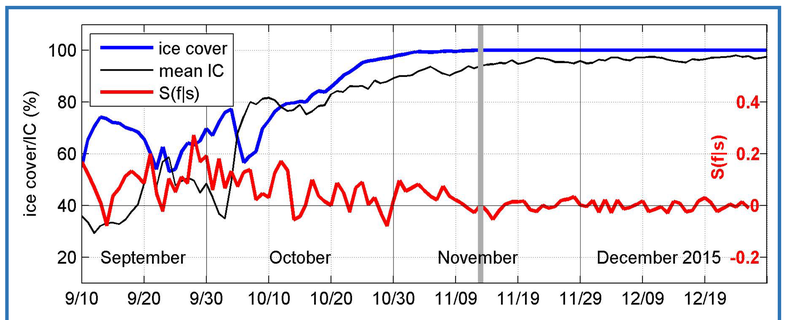

Fig. 1 24-hour skill wrt isotropic/homogeneous correlation model

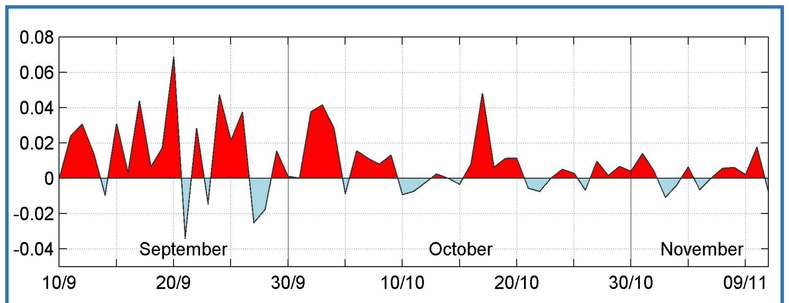

Fig. 2 24-hour skill wrt homogeneous correlation model in gaussianinzed case

ICE THICKNESS ASSIMILATION

Fig. 3 CICE ice thickness (contours) and CryoSat-2 observations (blue dots) on October 21, 2015. Yellow asterisks show locations of *in situ* measurements used for cross-validation.

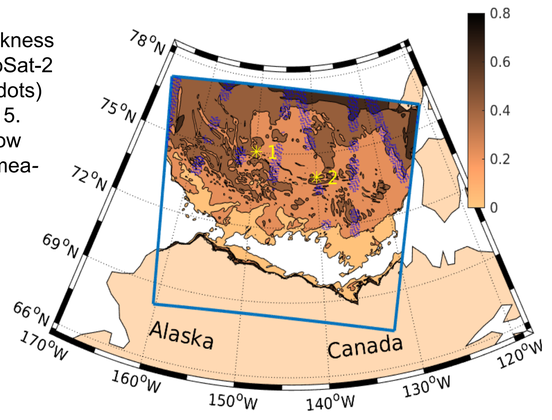

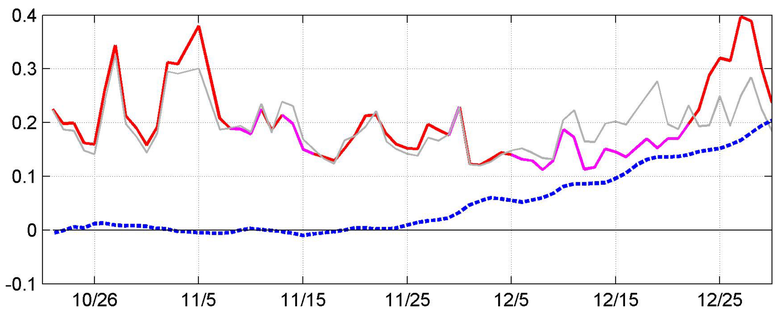

Fig. 4. Absolute value of the model-data misfits (meters) between the 24-hour forecasts produced by the runs with (gray line) and without (red/blue line) IT assimilation. Periods of the IT forecast improvement are shown in red. The dashed blue line shows difference in the mean IT between model runs without and with IT assimilation (CICE model tends to overestimate ice accumulation in the Beaufort Sea in December).

VALIDATION AGAINST *IN SITU* DATA

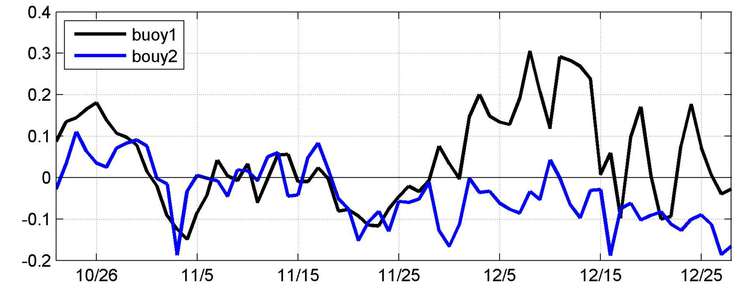

Fig. 5. The difference (m) between the model-data IT misfits in two buoys produced by the model runs with and without IT assimilation. Positive values correspond to smaller misfit of the assimilation run.

IMPACT OF GAUSSIANIZATION

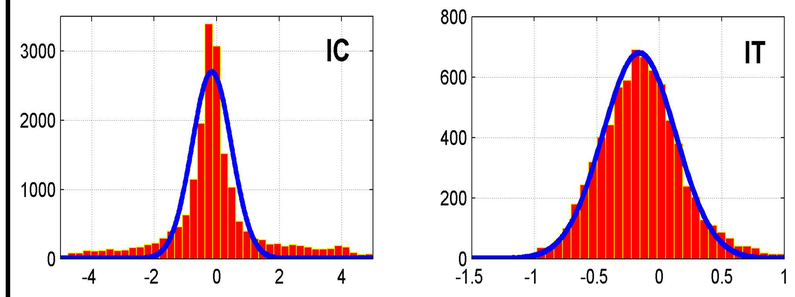

Fig. 6 Histograms of IC (25.09.2015) and IT (25.12.2015) innovations

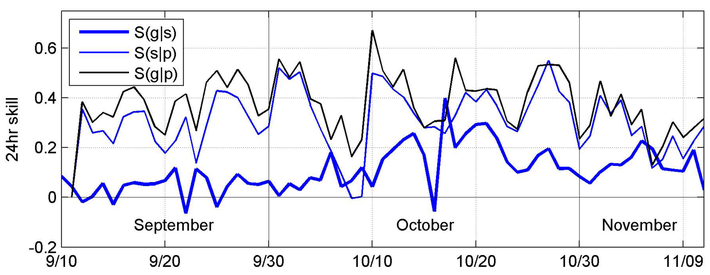

Fig. 7 The forecast skill wrt persistence of the operational (thin blue line) and gaussianized (thin black) runs. Thick blue line shows the forecast skill improvement due to gaussianization.

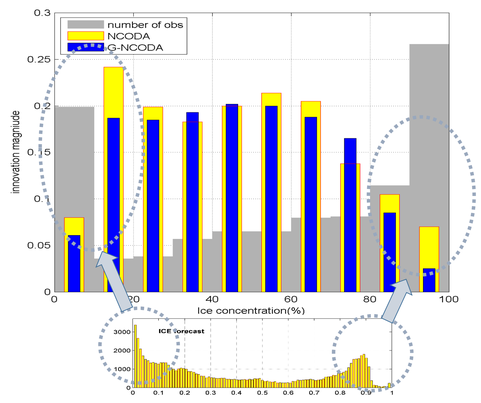

Fig. 8 Distribution of the space and time averaged innovation magnitudes over ten ice concentration cathegories for the operational run (yellow bars) and for the gaussianized run (blue bars). Grey bars show relative numbers of the respective observation points.

SUMMARY

1. Introduction of the flow-dependent correlations improves the forecast skill by 5-7% during the freezing period (September 10, 2015 - November 13, 2015) with no significant impact on the forecast skill later, when the area-mean IC becomes close to saturation.
2. Gaussianization contributes an additional improvement of 3-4% during the freezing period and has no effect on the skill after mid-November.
3. Introduction of the IT assimilation capability did not show any statistically significant improvement of the 24-hour forecast skill, because spatial separation between the daily CryoSat tracks is much larger than the respective dynamical propagation distance of the IT updates.
4. Comparison with independent *in situ* IT observations demonstrated only a minor (1-3 cm) improvement at a statistically insignificant level. At the same time, a much more noticeable (15-25%, or 3-11 cm) improvement was detected in the model's discrepancy with independent monthly mean AMSR-E IT data